Stepwise drying of Lake Turkana at the end of the African Humid Period: a forced regression modulated by solar activity variations?

Alexis Nutz[1], Mathieu Schuster[1]

Institut de Physique du Globe de Strasbourg (IPGS), UMR 7516, Centre National de la Recherche Scientifique, Université de Strasbourg, École et Observatoire des Sciences de la Terre, 1 rue Blessig, 67084 Strasbourg, France

**Corresponding author* (nutz@unistra.fr)

Running head: Lake Turkana drying at the end of the AHP

Keywords: East African Rift System; Turkwel delta; Lake-level; Holocene; Solar activity

Abstract

Although timing of the termination of the African Humid Period (AHP) is now relatively well-established, modes and controlling factors are still being debated. Here, through a geomorphological approach, we characterize the evolution of the final regression of Lake Turkana at the end of the AHP. We show that lake level fall during this period was not continuous but stepwise and consisted of five episodes of rapid lake-level fall separated by episodes of slower rates of lake-level fall. Whereas the overall regressive trend can be attributed to decreasing regional precipitations due to the gradual reduction in northern hemisphere summer insolation controlled by orbital precession, we focus discussion on the origin of the five periods of accelerated lake-level fall. We propose that these are due to temporary reductions in rainfall across Lake Turkana area associated with repeated westward displacement of the Congo Air Boundary (CAB) during minima in solar activity.

1. Introduction

The African Humid Period (AHP), *c*. 14.8 to 5.5 ka cal BP, is a major climate period that was paced by orbital parameters (i.e. precession) (deMenocal et al., 2000; deMenocal and Tierney, 2012; Bard, 2013; Shanahan et al., 2015) and that markedly impacted environment, ecosystems, and human occupation of Africa over several millennia (Bard, 2013). An increase in rainfall during this climate period led to the rise and highstand of numerous African lakes (Street and Grove, 1976; Tierney et al., 2011). The end of the AHP was characterized by the establishment of more arid conditions, leading to dramatic lake level falls (Street-Perrott and Roberts, 1983; Kutzbach and Street-Perrott, 1985). This aridification forced Neolithic populations to adapt to more limited resources (Kuper and Kröpelin, 2006) and represents a recent example of major climate change. The mid-Holocene termination of the AHP is thought to have been either abrupt (deMenocal et al., 2000), gradual (Kröpelin et al., 2008) or time-transgressive (Shanahan et al., 2015) depending on location, an ongoing debate highlighting the variable responses of proxies to dominant forcings and the complex interactions among the multiple components of the local environment (e.g., deMenocal, 2000; Renssen et al., 2006; Liu et al., 2007; Tierney and deMenocal, 2013; Shanahan et al., 2015). However, drying trends remains poorly-constrained and as a consequence the final regressions of African lakes are presented at relative constant rate of lake level fall (e.g., Garcin et al., 2012; Forman et al., 2014; Morrissey and Scholz, 2014; Junginger et al., 2014; Bloszies et al., 2015). In this study, we investigate the drying trend of Lake Turkana and evidence for the first time that the final regression was not continuous through time revealing a more complex process than previously envisaged. Thus, understanding the mode of African lake regressions appears as particularly relevant in the context of projecting future global climate change impacts on the African continent (e.g., Patricola and Hook, 2011), especially in term of evolution of water resources from large lakes.

Lake Turkana is one of the great lakes of the East African Rift. It is considered as a Wind-driven Waterbody (Nutz et al., in press) that developed abundant wave-dominated coastal features all along its shoreline. These coastal features represent a valuable paleohydrological archives that contributes to the understanding of the evolution of Lake Turkana during the AHP (Garcin et al., 2012, Forman et al., 2014; Bloszies et al., 2015). However, the detailed and continuous evolution of lake level during the final forced regression (i.e., basinward migration of the shoreline associated with a base-level fall) marking the end of the AHP has not been already documented. Here, the delta complex of the Turkwel River (Fig. 1) that developed during the final forced regression of Lake Turkana is examined using trajectory analysis (Helland-Hansen and Hampson, 2009). Finally, we highlight variations in the rate of lake level fall during the regression. We interpret those variations as markers reflecting variable rate of decrease in precipitation during the crucial period corresponding to the terminal phase of the AHP. Subsequently, we discuss potential forcings responsible for the regressive pattern of Lake Turkana with a primary focus on the role of the Sun and short-term variability of insolation.

2. Materials and methods

The data set is comprised of satellite imagery and a digital elevation model (DEM). A recently obtained SRTM1 (Shuttle Radar Topography Mission (Rabus et al., 2003)) is available for the entire Lake Turkana area. This DEM is produced by radar interferometry with a one arcsec (approximately 30 m) horizontal grid spacing and an approximately 5 m absolute vertical error (Rosen et al., 2001; Tighe and Chamberlain, 2009). In addition, high-resolution (<1 m) PLEIADES and (5 m) SPOT 5 images (©CNES 2012, Airbus DS/ SPOT Image) were used to focus on selected areas. This data set was processed using GIS software (Global Mapper 15 software; Blue Marble Geographics, Hallowell, ME, USA) to provide a high-resolution 3D view of the geomorphological features. Topographic profiles, elevation differences, and slope values used for the trajectory analyses were obtained using Global Mapper 15 software.

3. Chronological framework

Humid conditions related to the AHP broadly prevailed over Africa from 14.8 to 5.5 ka cal BP (deMenocal et al., 2000; Shanahan et al., 2015). Several lake level curves associated with Lake Turkana evolution provide records of the regional moisture history over the Holocene (Garcin et al., 2012; Forman et al., 2014; Bloszies et al., 2015). Based on surveys of raised Holocene beach ridges coupled with dated archeological sites, these studies provide a relatively robust chronological framework for the final regression at the end of the AHP. Garcin et al. (2012) initially estimated the onset of the final lake level fall in Lake Turkana at *c*. 5.27 ± 0.36 ka cal BP. Subsequently, Forman et al. (2014) proposed that the age of this final regression occurred between 5.5/5.0 to 4.6 ka cal BP associated with a lake level change from 440 to 380 m asl. Finally, Bloszies et al. (2015) proposed an onset of the final regression of the AHP starting at 5.18 ± 0.12 ka cal BP (dating of a shell at 90 m above the modern Lake Turkana) and finishing at 4.58 ± 0.25 ka BP (OSL age reused from Forman et al., 2014; sample UIC2319) associated with a lake level grading from 450 to 375 m asl. Based on these published data, we carried out minor complementary processing in order to refine the chronology. First, we recalibrated sample (SNU12-589) considered to provide the age of the onset of the final regression. Using a most recent curve (INTCAL13; Reimer et al., 2013), the onset of the final regression is now given at 5.14 ± 0.18 ka cal BP (4.51 ± 0.06 ka ^{14}C BP). Second, we converted the OSL age (4.58 ± 0.25 ka BP; sample OSL23/1.30) that is considered to represent the end of the final regression (Forman et al., 2014) in radiocarbon age. Indeed, Forman et al. (2014) provided 6 samples that were dated by both OSL and radiocarbon methods. Even the limited number of samples, we then processed a linear regression in order to propose a statistic relationship between OSL and radiocarbon ages. At the end, based on this correlation ($age_{(OSL)}=0.98386063*age_{(^{14}C(calibatred))}$; b(the intercept) has been forced to 0; $r^2=0.9942$), the age of the end of the final regression is now estimated at 4.65 ± 0.3 ka cal BP (4.14 ± 0.24 ka ^{14}C BP). As such, based on thise most recent available age-model, the final regression of Lake Turkana at the end of the AHP would, at the longest, span a period from 5.32 to 4.35 ka cal BP. At a minimum, the final regression would have occurred between 4.96 and 4.95 ka cal BP. This implies a duration ranging between 10 to 1030 years, with a mean duration of 510 years for water level to decrease from the Holocene highstand (450 m asl) to the lowstand (375 m asl). Considering the largest potential time interval during which the final regression occurred (i.e., interval between 4.57 and 3.90 ka ^{14}C BP), a mean age of 4.23 ± 0.33 ka ^{14}C BP is established in order to allow a calibration and then to provide a probability curve. At the end, calibration reveals a 44% of probability that the final regression precisely occurred between 5.14 ± 0.18 and 4.65 ± 0.3 ka cal BP. Because the investigated portion of the Turkwel delta is located between 450 and 375 m asl, ages of the landforms are considered to have developed between 5.14 ± 0.18 and 4.65 ± 0.3 ka cal BP.

4. Geomorphological analysis

The Turkwel delta complex is 35 km long, forming one of the major deltaic systems that fringed Lake Turkana during the Holocene (Fig. 1). It was developed as the shoreline migrated basinward, lowering from 450 to 360 m asl (Fig. 2). From west to east, five distinct progradational stages were identified (Fig. 2d). The first progradational stage forms a lobe protruding out from the mean north–south paleoshoreline, well defined by the 450 m asl elevation shoreline (red line in Fig. 2d). According to regional age models (Garcin *et al.*, 2012; Forman et al., 2014; Bloszies et al., 2015), this first progradational stage marks the last

Holocene highstand before the end of the AHP. Moving eastward, each of the three topographic profiles cross-cutting the Turkwel delta complex (Fig. 3) shows five slightly inclined plateaus interrupting at *c.* 445, 425, 410, 400 and 390 m asl, respectively, separated by five abrupt 5-to 15-m-high steps (Fig. 4). Each plateau defines a different progradational stage. The plateaus are 3- to 5-km-wide, and correspond to successively abandoned delta plains (Fig. 2d). To the north, these plateaus systematically end with paleo-spits that document ancient, northward-flowing alongshore currents. The resulting landform reveals the Turkwel delta complex as composed of successive asymmetric wave-dominated deltas (Bhattacharya and Giosan, 2003; Anthony 2015) during most of its evolution, except in the early period associated with the AHP highstand. None of the plateaus exhibit any evidence of significant erosion that would indicate reworking of the landforms subsequent to their deposition, except for the fluvial incision of the Turkwel River that progressively adjusted to the base level fall. This supports the Turkwel delta complex as a primary depositional landform corresponding to a continuous, comprehensive record of lake level evolution.

Trajectory analysis, performed for the three transects that cross-cut the Turkwel delta complex along its progradation axis (Fig. 3), reveals that the plateaus are continuous, having slightly descending regressive trajectories (slope gradient: >0° to 0.4°). The five abrupt steps that separate plateaus have much higher slope gradients (1° to 3.8°), and are also defined as descending regressive trajectories. Trajectories reflect a progradation associated with a general lake level fall that meets the definition of a forced regression (Posamentier *et al.*, 1992). Moreover, the five abrupt steps reflect recurrent, short-lived increases in the rate of lake level fall that evidence a stepwise forced regression at the end of the AHP. In order to confirm this interpretation, we investigated another portion of the Lake Turkana paleoshoreline. In the eastern Omo River valley (Fig. 1), topographic profiles along two fossil spits are presented (Fig. 5). The two spit systems show successive plateaus at elevations (*c.*

445, 425, 410 and 400 m asl) similar to those observed in the Turkwel delta complex (Fig. 3). Finally, these additional observations firmly support the reconstructed evolution of lake level deduced from the Turkwel delta complex. The overall trend of the three transects in the Turkwel delta as well as transects in the fossil spits of the eastern Omo River valley lend support to the idea of a stepwise final, forced regression of Lake Turkana at the end of the AHP.

5. Discussion

5.1. Origin of Lake Turkana lake level evolution

Lake level fluctuations may result from changes in the quantity of water supply to a lake, from altered evapotranspiration rates within the catchment area, or from modifications in basin physiography. These changes may originate from a number of potential external forcing processes, among which the most commonly considered are tectonism and climate. Tectonism may be ruled out as the origin of any physiographic modification of the Lake Turkana basin that would have caused abrupt falls in lake level at such time-scale. Vertical crustal movements occur over much longer time periods than that of the AHP termination and the rate of subsidence in the basin is too low (i.e. $0.4\ \mathrm{m{\cdot}ka^{-1}}$ at the Eliye Spring well site (Morley *et al.*, 1999)), to explain several lake level falls of >5 m each in maximum 1000 years. Moreover, vertical displacements at this scale would require earthquakes having a magnitude >9 (Pavlides and Caputo, 2004). Earthquakes of this magnitude are unknown in the area and are not compatible with rift systems. Finally, volcanism event is known to have occurred (Karson and Curtis, 1994) during the Late Quaternary even the age is not very-well constrained. However, repeated pulsed of accelerated subsidence related to successive emptying of a magma chamber is prevented by the insufficient amount of magma observed in the basin. Indeed, no regional magmatic effusion that would have caused sudden subsidence is observable. Magmatism rather corresponds to punctual effusion forming the north, central, and south islands. As such, the abrupt nature of the accelerated lake level falls can be attributed only with difficulty to tectonics and magmatism leaving climate variability as the most likely forcing mechanism.

During the Holocene, the overall climate pattern in East Africa was governed by insolation changes related to changes in precessional orbital parameters of the Earth (Barker et al., 2004). Links between insolation and hydrology are now well established for this region, in particular monsoonal rainfall intensity that is strongly correlated with summer insolation (deMenocal et al., 2000; Shanahan et al., 2015). In the early Holocene, an increase in summer insolation due to changing orbital parameters produced wetter conditions over much of the African continent leading to the establishment of the AHP. Subsequently, the overall contraction of lakes at the end of the AHP is generally attributed to decreased precipitation related to a reduction of summer insolation (deMenocal et al., 2000; Shanahan et al., 2015) controlled by orbital parameters (i.e. precessional forcing; deMenocal and Tierney, 2012; Bard, 2013). Therefore, changes in insolation imply additional modifications in rainfall amounts through the strengthening or weakening of local climate processes. In the Lake Turkana area, Junginger et al. (2014) suggest that the increase of precipitation during the AHP is mainly a result of a north-eastward shift of the Congo Air Boundary (CAB). The CAB is a north-east to south-west oriented convergence zone presently located west of the Lake Turkana area. This convergence zone shifts eastward in response to an enhanced atmospheric pressure gradient between India and East Africa during northern hemisphere insolation maxima (Junginger and Trauth, 2013; Junginger et al., 2014). When the CAB moves eastward over the Turkana area, precipitation is expected to increase significantly. Because the five abrupt accelerations in lake level fall require short-term accentuated decreases in precipitation, we propose that these five periods of significantly reduced rainfall amounts are related to short-term decreases of insolation that repeatedly moved the CAB position. At such decadal to centennial time-scale, variations of solar activity appear as the most likely acting parameter to explain variations in insolation. This potential origin needs to be discussed.

5.2. Linking solar activity and paleohydrology

Links between short-term (decadal-scale) solar activity and climate change remains a point of debate. However, periodicities in solar activity such as the 11-year sunspot cycle, the Gleissberg cycle (80—90 years) (Peristykh and Damon, 2003) or the de Vries cycle (~200 years) (Raspopov et al., 2008) have been identified in Holocene paleoenvironmental records and suggests a possible forcing by solar activity on climate (Crowley, 2000; Bond et al., 2001; Gray et al., 2013). Especially in Lake Turkana, the potential expression of the 11-year sunspot cycle has already been deciphered through time-series analysis for sediments associated with the last 4 ka (Halfman et al., 1994). Within some African lakes, several authors link more arid periods with solar activity minima (Stager et al., 2002 and Junginger et al., 2014) and Lake Turkana is one of them. The capacity of those lakes to record changes in paleohydrology attributed to variations in solar activity may rely to the fact that these lakes are very sensitive. Indeed, they are considered as “amplifier lakes” (Street-Perrott and Harrison, 1985) for which relatively modest changes in climate are amplified into significant lake-level fluctuation due to their specific morphology. As an amplifier lake, Lake Turkana could be more sensitive to precipitation changes from small variations in insolation as those generated by modifications in solar activity.

Coupling the proposed chronological framework with the solar activity curve from Steinhilber et al. (2009), we observed in the Lake Turkana between two and ten solar activity minima during the minimum and maximum potential period of regression, respectively (Fig.6). Considering a mean time of 510 years given by the age-model during which the final regression occurred, five solar activity minima are observed. The number of these minima interestingly matched with the number of abrupt lake level falls suggesting a possible link between the short-term variability of solar activity and the lake level changes in Lake Turkana at the end of the AHP. Because a mechanism must be given, we propose that periods of solar activity maxima would be able to compensate for the precession-induced reduction of insolation. The relatively limited reduction of insolation would have led to a relatively stable position for the CAB over the Lake Turkana area and, in turn, a reduced rate of lake level fall due to slowly decreased precipitation amounts. However, when short-term solar activity minima are coupled with the precession-related insolation decrease, the CAB would have migrated rapidly westward resulting in drastic reduction of rainfall and as a consequence, a rapid fall in lake level. As such, alternations of solar activity maxima and minima could explain the geomorphological pattern that revealed a long-term fall in lake level interspersed by short-term accelerations in the rate of lake level fall during the final forced regression at the end of the AHP.

6. Conclusion

Geomorphic analysis (i.e. trajectory analysis) revealed for the first time a stepwise lake level fall of Lake Turkana during its final forced regression at the end of the AHP. Five rapid falls in lake level were identified, intercalated with periods of slower lake level fall. We suggest that the abrupt, short-term accelerations of lake level fall may be associated with insolation minima altering the position of the CAB, responsible for regional precipitation pattern. Our interpretation suggests that short-term variability of insolation, due to variability in solar activity, may have influenced the hydroclimatic conditions in the Turkana area during the final forced regression of the AHP. Next step would be to correlate each paleo plateaus to a specific solar maxima and each step to a specific minima. Nevertheless, uncertainties of dating methods will allow only with difficulty to provide enough precise ages for such features developed at the decadal to centennial time-scale.

Acknowledgements

This works is a contribution of the Rift Lake Sedimentology project (RiLakS) funded by Total Oil Company. Satellite images (SPOT and PLEIADES) were acquired thanks to the support of CNES/ISIS program. Finally, we are grateful to Murray Hay (Maxafeau Editing Services) for verification of the English text.

References

Anthony, E.J.: Wave influence in the construction, shaping and destruction of river, Mar. Geol. 361, 53–78, 2015.

Bard, E.: Out of the African Humid Period, Science, 342, 808–809, 2013.

Barker, P.A., Talbot, M.R., Street-Perrott, F.A., Marret, F., Scourse, J. and Odada, E.O.: Late Quaternary climatic variability in intertropical Africa, in: Past Climate Variability through Europe and Africa (R.W. Battarbee, F. Gasse, C.E. Strickley, eds) Springer, Dordrecht, 2004.

Bhattacharya, J.P. and Giosan, L.: Wave-influenced deltas: geomorphological implications for facies reconstruction, Sedimentology, 50, 187–210, 2003.

Bloszies, C., Forman, S.L. and Wright, D.K.: Water level history for Lake Turkana, Kenya in the past 15,000 years and a variable transition from the African Humid Period to Holocene aridity, Glob. Planet. Change, 132, 64–76, 2015.

Bond, G., Kromer, B., Beer, J., Muscheler, R., Evans, M.N., Showers, W., Hoffman, S., Lotti-Bond, R., Hajdas, I. and Bonani, G.: A pervasive millennial-scale cycle in North Atlantic Holocene and glacial climates, Science, 278, 1257–1266, 2001.

Crowley, T.: Causes of climate change over the past 1000 years, Science, 289, 270–277, 2000.

deMenocal, P.B. and Tierney, J.E.: Green Sahara: African Humid Periods paced by Earth's orbital changes, Nature Educ. Knowl., 3, 12, 2012.

deMenocal, P.B., Ortiz, J., Guilderson, T., Adkins, J., Sarnthein, M., Baker, L. and Yarusinsky, M.: Abrupt onset and termination of the African Humid Period: rapid climate responses to gradual insolation forcing, Quat. Sci. Rev., 19, 347–361, 2000.

Forman, S.L., Wright, D.K. and Bloszies, C.: Variations in water level for Lake Turkana in the past 8500 years near Mt. Porr, Kenya and the transition from the African Humid Period to Holocene aridity, Quat. Sci. Rev., 97, 84–1014, 2014.

Garcin, Y., Melnick, D., Strecker, M.R., Olago, D. and Tiercelin, J.-J.: East African mid-Holocene wet-dry transition recorded in palaeo-shorelines of Lake Turkana, northern Kenya Rift, Earth Planet. Sci. Lett., 331–322, 322–334, 2012.

Gray, L., Scaife, A.A., Mitchell, D.M., Osprey, S., Ineson, S., Hardiman, S., Butchart, N., Knight, R., Sutton, R., and Kodera, K.: A lagged response to the 11-year solar cycle in observed winter Atlantic/European weather patterns, J. Geophys. Res., 118, 13405–13420, 2013.

Halfman, J.D., Johnson, T.C. and Finney, B.P.: AMS dates, stratigraphic correlations and decadal climatic cycles for the past 4 ka at Lake Turkana, Kenya, Palaeogeog. Palaeoclimatol. Palaeoecol, 111, 83-98, 1994

Helland-Hansen, W. and Hampson, G.: Trajectory analysis: concepts and application, Basin Res., 21, 454–483, 2009.

Junginger, A., Roller, S., Olaka, L.A. and Trauth, M.H.: The effects of solar irradiation changes on the migration of the Congo Air Boundary and water levels of paleo-Lake Suguta, Northern Kenya Rift, during the African Humid Period (15–5 ka BP), Palaeogeog. Palaeoclimatol. Palaeoecol, 396, 1–16, 2014.

Junginger, A. and Trauth, M.H.: Hydrological constraints of paleo-Lake Suguta in the Northern Kenya Rift during the African Humid Period (12–5 ka BP), Glob. Planet. Change, 111, 174–188, 2013.

Karson, J.A., and Curtis, P.C.: Quaternary volcanic centres of the Turkana Rift, Kenya: Journal of African Earth Sciences, 18, 15–35, 1994.

Kröpelin, S., Verschuren, D., Lézine, A.-M., Eggermont, H., Cocquyt, C., Francus, P., Cazet, J.-P., Fagot, M., Rumes, B., Russell, J.M., Darius, F., Conley, D.J., Schuster, M., von Suchodoletz, H. and Engstrom, D.R., : Climate-driven ecosystem succession in the Sahara: The past 6000 years, Science, 320, 765–768, 2008.

Kutzbach, J.E., and Street-Perrott, F.A.: Milankovitch forcing of fluctuations in the level of tropical lakes from 18 to 0 kyr BP, Nature, 317, 130–134, 1985.

Kuper, R. and Kröpelin, S.: Climate-controlled Holocene occupation in the Sahara: Motor of Africa's evolution, Science, 313, 803–807, 2006.

Liu, Z., Wang, Y., Gallimore, R., Gasse, F., Johnson, T., deMenocal, P., Adkins, J., Notaro, M., Prentice, I.C., Kutzbach, J., Jacob, R., Behling, P., Wang, L. and Ong, E.: Simulating the transient evolution and abrupt change of Northern Africa atmosphere-ocean-terrestrial ecosystem in the Holocene, Quat. Sci. Rev., 26, 1818–1837, 2007.

Morley, C.K., Karanja, F.M., Wescott, W.A., Stone, D.M., Harper, R.M., Wigger, S.T. and Day, R.A.: Geology and geophysics of the western Turkana basins, Kenya. Am. Assoc. Petrol. Geol., 44, 19–54, 1999.

Morrissey, A., and Scholz, C.A.: Paleohydrology of Lake Turkana and its influence on the Nile River system: Palaeogeog. Palaeoclimatol. Palaeoecol, 403, 88–100, 2014.

Nutz A., Schuster, M., Ghienne, J-F., Roquin C and Bouchette F, accepted in Journal of Paleolimnology, special publication ILIC 6. Wind-driven Waterbodies: A new category of lake within an alternative sedimentologically-based lake classification.

Patricola, C.M. and Hook, K.H.: Sub-Saharan Northern African climate at the end of the twenty-first century: Forcing factors and climate change processes, Clim. Dyn., 37, 1165–1188, 2011.

Pavlides, S. and Caputo, R.: Magnitude versus faults' surface parameters: quantitative relationships from the Aegean Region. Tectonophysics, 380, 159–188, 2004.

Peristykh, A.N. and Damon P.E.: Persistence of the Gleissberg 88-year solar cycle over the last 12 000 years: Evidence from cosmogenic isotopes, J. Geophys. Res., 108, A1, 2003.

Posamentier, H.W., Allen, G.P., James, D.P. and Tesson, M.: Forced regressions in a sequence stratigraphic framework: concepts, examples, and exploration significance. Am. Assoc.Petrol. Geol. Bull., 76, 1687–1709, 1992.

Rabus, B., Eineder, M., Roth, A. and Bamler, A.: The shuttle radar topography mission - a new class of digital elevation models acquired by spaceborne radar. ISPRS J. Photogram. Rem. Sens., 57(4), 241–262, 2003.

Raspopov O.M., Dergachev, V.A., Esper, J., Kozyreva, O.V., Frank, D., Ogurtsov, M., Kolström, T. and Shao, X.: The influence of the de Vries (200-years) solar cycle on climate variations: Results from the Central Asian Mountains and their global link, Palaeogeog. Palaeoclimatol. Palaeoecol., 259, 6–16, 2008.

Reimer, P.J., Bard, E., Bayliss, A., Beck, J.W., Blackwell, P.G., Bronk Ramsey, C., Buck, C.E., Cheng, H., Edwards, R.L., Friedrich, M., Grootes, P.M., Guilderson, T.P., Haflidason, H., Hajdas, I., Hatté, C., Heaton, T.J., Hoffmann, D.L., Hogg, A.G., Hughen, K.A., Kaiser, K.F., Kromer, B., Manning, S.W., Niu, M., Reimer, R.W., Richards, D.A., Scott, E.M., Southon, J.R., Staff, R.A. and Turney, C.S.M., INTCAL13 and MARINE13 radiocarbon age calibration curves, 0-50,000 years Cal BP: Radiocarbon, 55, 1869-1887, 2013

Renssen, H., Brovkin, V., Fichefet, T. and Goosse, H.: Simulation of the Holocene climate evolution in Northern Africa: The termination of the African Humid Period, Quat. Inter., 150, 95–102, 2006.

Shanahan, T.M., McKay, N.P., Hughen, K.A., Overpeck, J.T., Otto-Bliesner, B., Heil, C.W., King, J., Scholz, C.A. and Peck, J.: The time-transgressive termination of the African Humid Period, Nature Geosci., 8, 140–144, 2015.

Stager, J.C., Mayewski, P.A. and Meeker, L.D.: Cooling cycles, Heinrich event 1, and the desiccation of Lake Victoria, Palaeogeog. Palaeoclimat. Palaeoecol., 183, 169–178, 2002.

Tighe, M.L. and Chamberlain, D.: Accuracy comparison of the SRTM, ASTER, NED, NEXTMAP USA digital terrain model over several USA study sites, ASPRS/MAPPS Fall Conference, November 16-19, 2009.

Steinhilber, F., Beer, J. and Fröhlich, C.: Total solar irradiance during the Holocene, Geophys. Res. Lett., 36, L19704, 2009.

Street-Perrott, F.A. and Harrison, S.P.: Lake levels and climate reconstruction, Paleoclimate analysis and modeling, 291–340, 2009, 1985.

Street-Perrott, F.A. and Roberts, N.: Fluctuations in closed basin lakes as indicators of past atmospheric circulation patterns, in: Street-Perrott, F.A., Beran, M., and Ratcliffe, R.A.S., ed., Variations in the global water budget: Dordrecht. Reidel. 331–345, 1983

Street, F.A. and Grove, A.T.: Environmental and climatic implications of late Quaternary lake level fluctuations in Africa, Nature, 261, 385–390, 1976.

Tierney, J.E. and deMenocal, P.: Abrupt shifts in Horn of Africa hydroclimate since the Last Glacial Maximum, Science, 342, 843–846, 2013.

Tierney, J.E., Lewis, S.C., Cook, B.I., LeGrande, A.N. and Schmidt, G.A.: Model, proxy and isotopic perspectives on the East African Humid Period, Earth Planet. Sci. Lett., 307, 103–112, 2011.

FIGURE CAPTIONS

Figure 1. Location maps. (a) Lake Turkana basin in the East African Rift System (EARS). (b) Digital elevation model (DEM) SRTM1 showing Lake Turkana and the two considered areas (Turkwel delta and the east side of the Omo River valley). Dashed white line represents the maximum Holocene lake level. All described geomorphological features are located between the paleolake limit and the modern lakeshore.

Figure 2. Turkwel delta complex. (a) Raw digital elevation model SRTM1 of the Turkwel delta. (b) Slope direction shading applied to the DEM SRTM1 of the Turkwel delta to highlight the steps separating the different plateaus. Markers display the correspondence

between the DEM SRTM1 and the slope direction shading (see (a)). (c) SPOT5 satellite image of the Turkwel delta. (d) Interpretative geomorphological map of the area showing five successive delta plains in addition to the oldest plain associated with the late AHP highstand.

Figure 3. Geomorphological data for the Turkwel delta complex. (a) SRTM1 images were processed to display a digital elevation model of the Turkwel delta complex. Locations of the topographic transects are presented. (b) Topographic transects P1, P2, and P3. (c) Trajectory analyses show that the overall forced regressive trend (>0° to 0.4°) is punctuated by five steeper slopes (1° to 3.8°) revealing short-term increases in the rates of lake level fall.

Figure 4. Landforms from Turkwel delta. (a) Front view of a step grading downward to a plateau. (b) Side view of the same step separating two plateaus.

Figure 5. Sandspit systems, outlined by dashed white lines, along the eastern Omo River valley (location Fig.1b) from SRTM 1 (left side) and from PLEIADES images (right side). The sandspits display plateaus having similar elevations as those of the Turkwel delta.

Figure 6. The red curve presents total solar irradiance (40-year moving average) relative to the value of the PMOD composite during the solar cycle minimum of the year 1986 (1365.57 W.m^{2}) (Steinhilber et al., 2009) for the period contemporaneous with AHP regression of Lake Turkana. The shaded band represents 1σ uncertainty. The blue curve represents the precessional curve covering the same time period (http://www.imcce.fr/Equipes/ASD/insola/earth/online/). Grey stripes highlight solar activity minima.

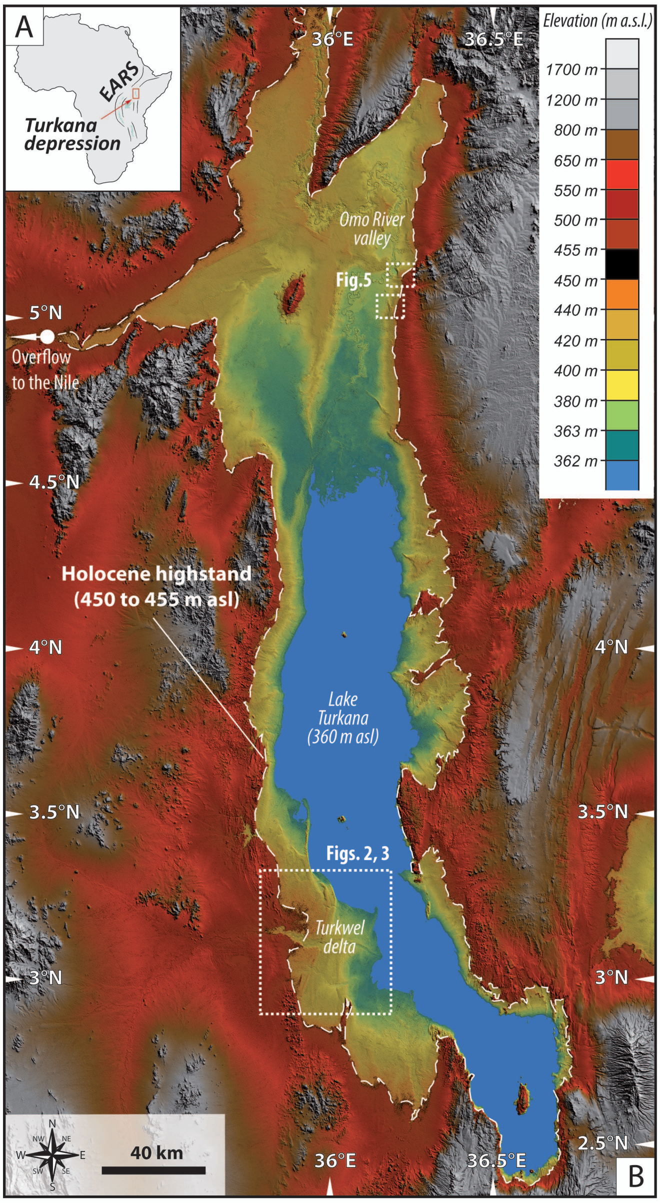
A
EARS
Turkana depression
36°E
36.5°E
Elevation (m a.s.l.)
1700 m
1200 m
800 m
650 m
550 m
500 m
455 m
450 m
440 m
420 m
400 m
380 m
363 m
362 m
Omo River valley
Fig.5
5°N
Overflow to the Nile
4.5°N
Holocene highstand (450 to 455 m asl)
4°N
4°N
Lake Turkana (360 m asl)
3.5°N
3.5°N
Figs. 2, 3
Turkwel delta
3°N
3°N
2.5°N
N
NW
NE
W
E
SW
SE
S
40 km
36°E
36.5°E
B

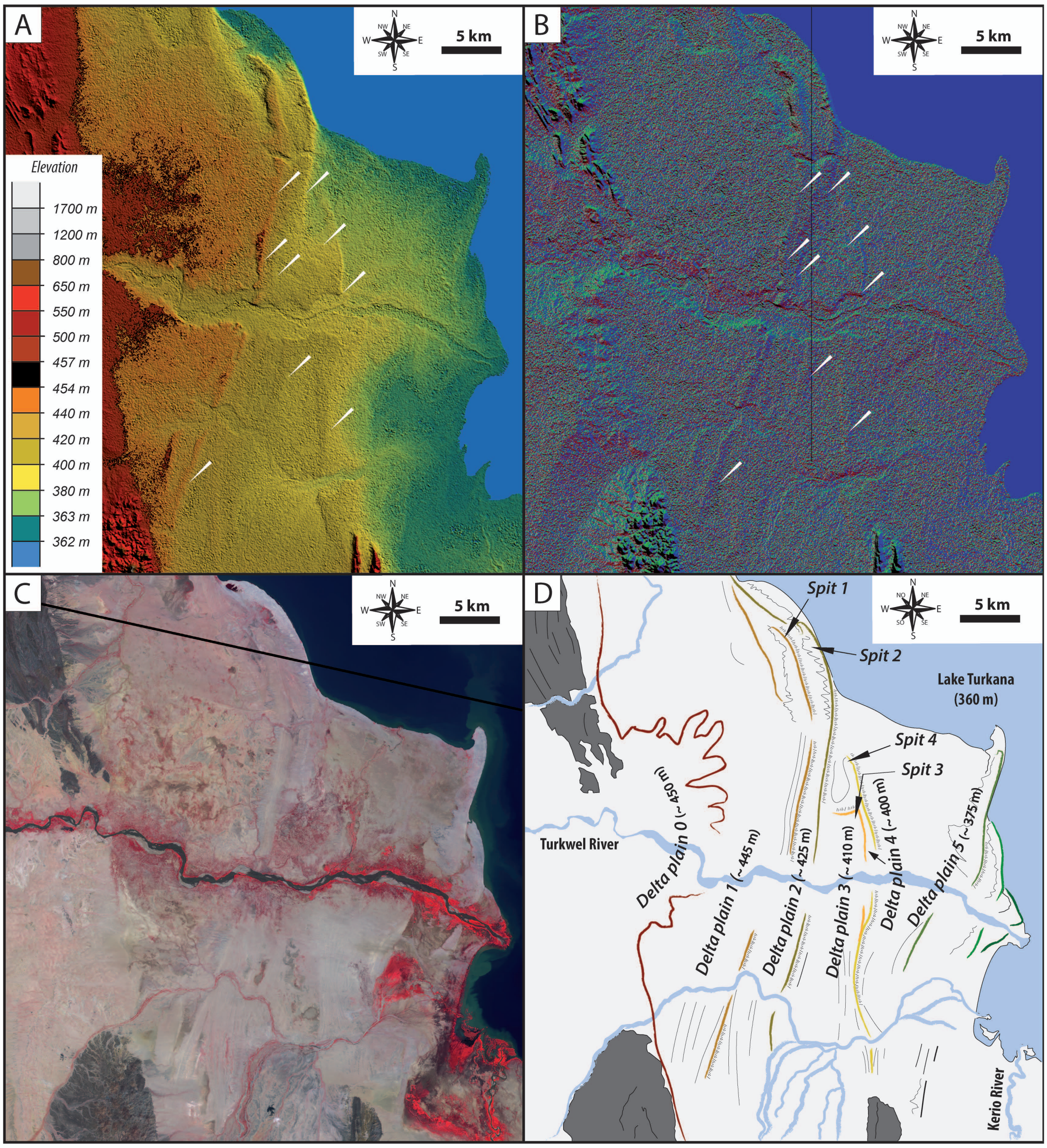
A
B
C
D
N
NW
NE
NO
W
E
SW
SE
SO
S
5 km
Elevation
1700 m
1200 m
800 m
650 m
550 m
500 m
457 m
454 m
440 m
420 m
400 m
380 m
363 m
362 m
Spit 1
Spit 2
Spit 3
Spit 4
Lake Turkana
(360 m)
Turkwel River
Kerio River
Delta plain 0 (~ 450 m)
Delta plain 1 (~ 445 m)
Delta plain 2 (~ 425 m)
Delta plain 3 (~ 410 m)
Delta plain 4 (~ 400 m)
Delta plain 5 (~ 375 m)

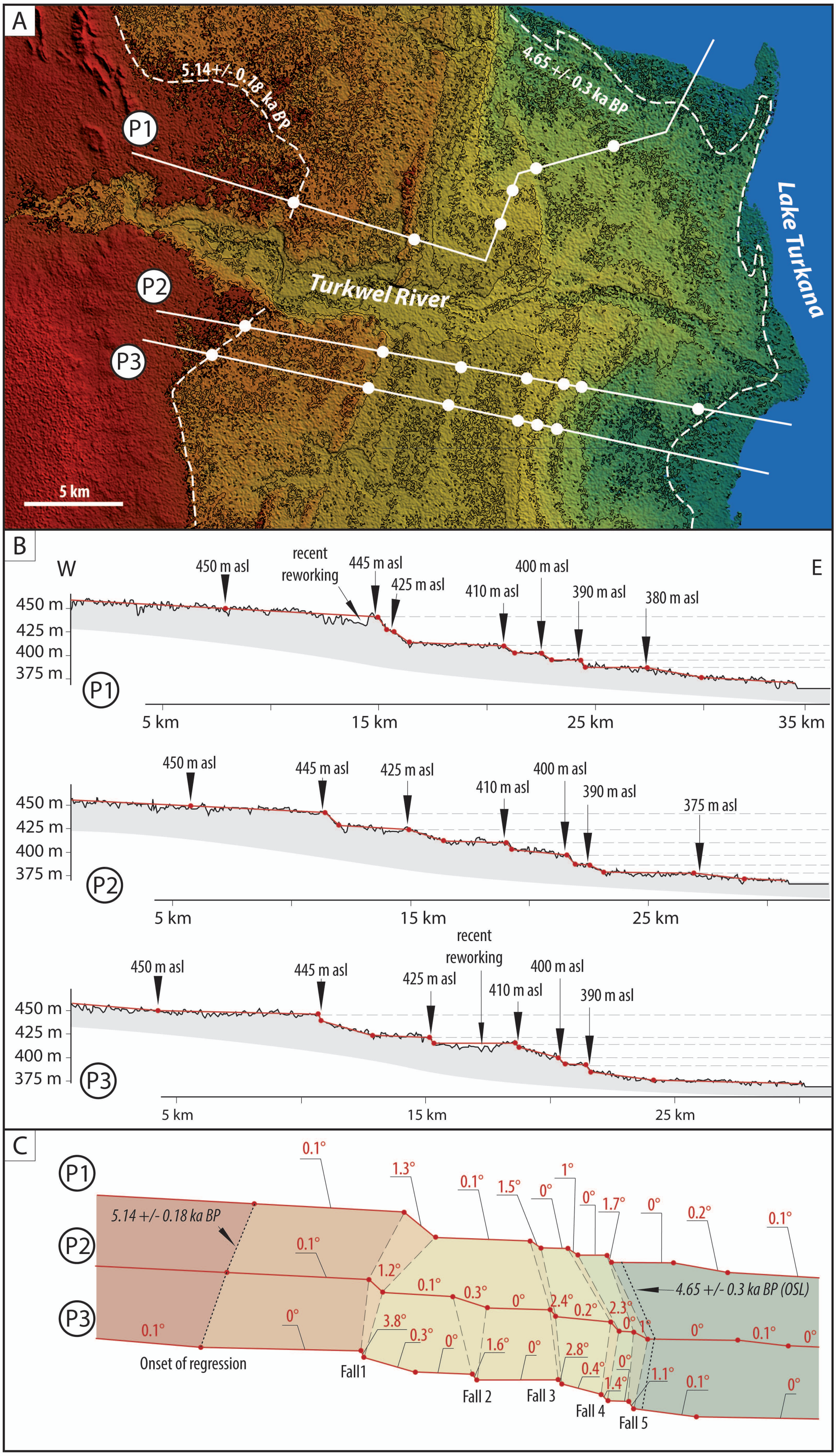
A
5.14+/- 0.18 ka BP
4.65 +/- 0.3 ka BP
P1
P2
P3
Turkwel River
Lake Turkana
5 km
B
W
E
450 m asl
recent reworking
445 m asl
425 m asl
410 m asl
400 m asl
390 m asl
380 m asl
450 m
425 m
400 m
375 m
P1
5 km
15 km
25 km
35 km
450 m asl
445 m asl
425 m asl
410 m asl
400 m asl
390 m asl
375 m asl
450 m
425 m
400 m
375 m
P2
5 km
15 km
25 km
450 m asl
445 m asl
425 m asl
recent reworking
410 m asl
400 m asl
390 m asl
450 m
425 m
400 m
375 m
P3
5 km
15 km
25 km
C
P1
P2
P3
5.14 +/- 0.18 ka BP
0.1°
1.3°
0.1°
1.5°
0°
1°
0°
1.7°
0°
0.2°
0.1°
0.1°
1.2°
0.1°
0.3°
0°
2.4°
0.2°
2.3°
0°
1°
0°
0.1°
0°
4.65 +/- 0.3 ka BP (OSL)
0.1°
0°
3.8°
0.3°
0°
1.6°
0°
2.8°
0.4°
0°
1.4°
1.1°
0.1°
0°
Onset of regression
Fall1
Fall 2
Fall 3
Fall 4
Fall 5

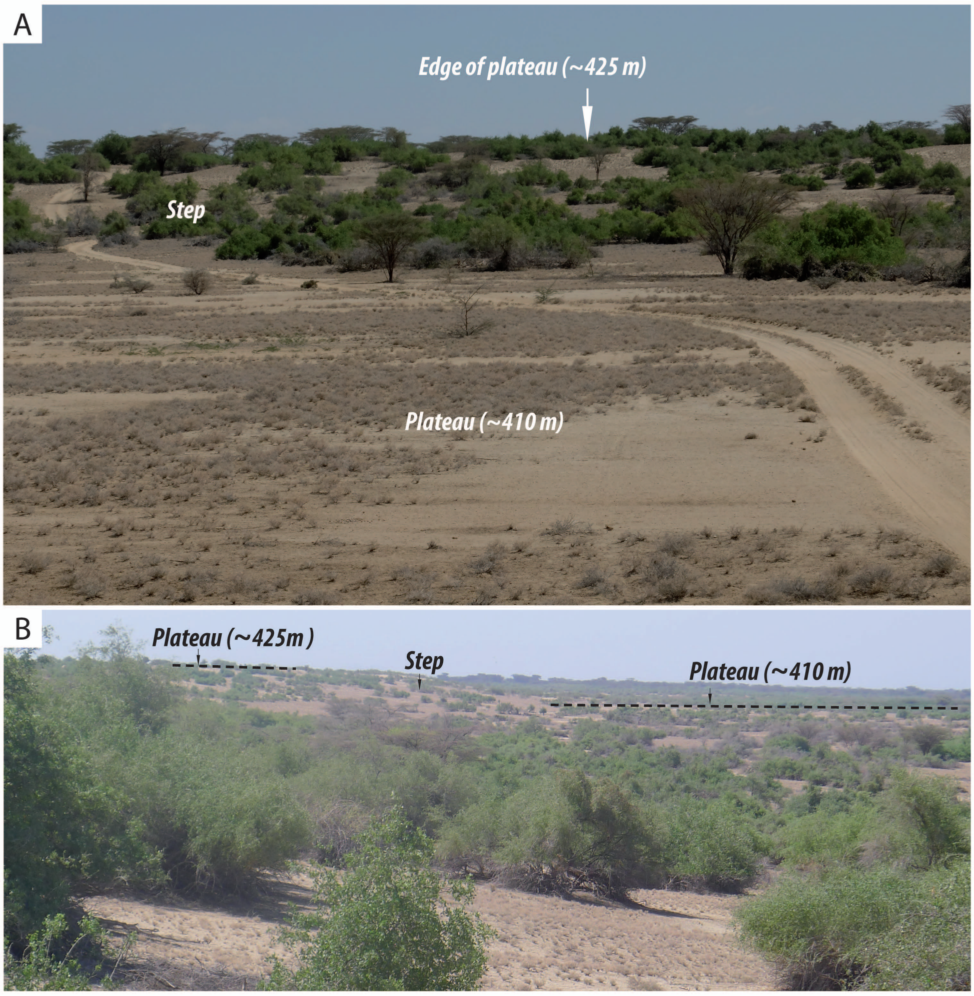
A
Edge of plateau (~425 m)
Step
Plateau (~410 m)
B
Plateau (~425m)
Step
Plateau (~410 m)

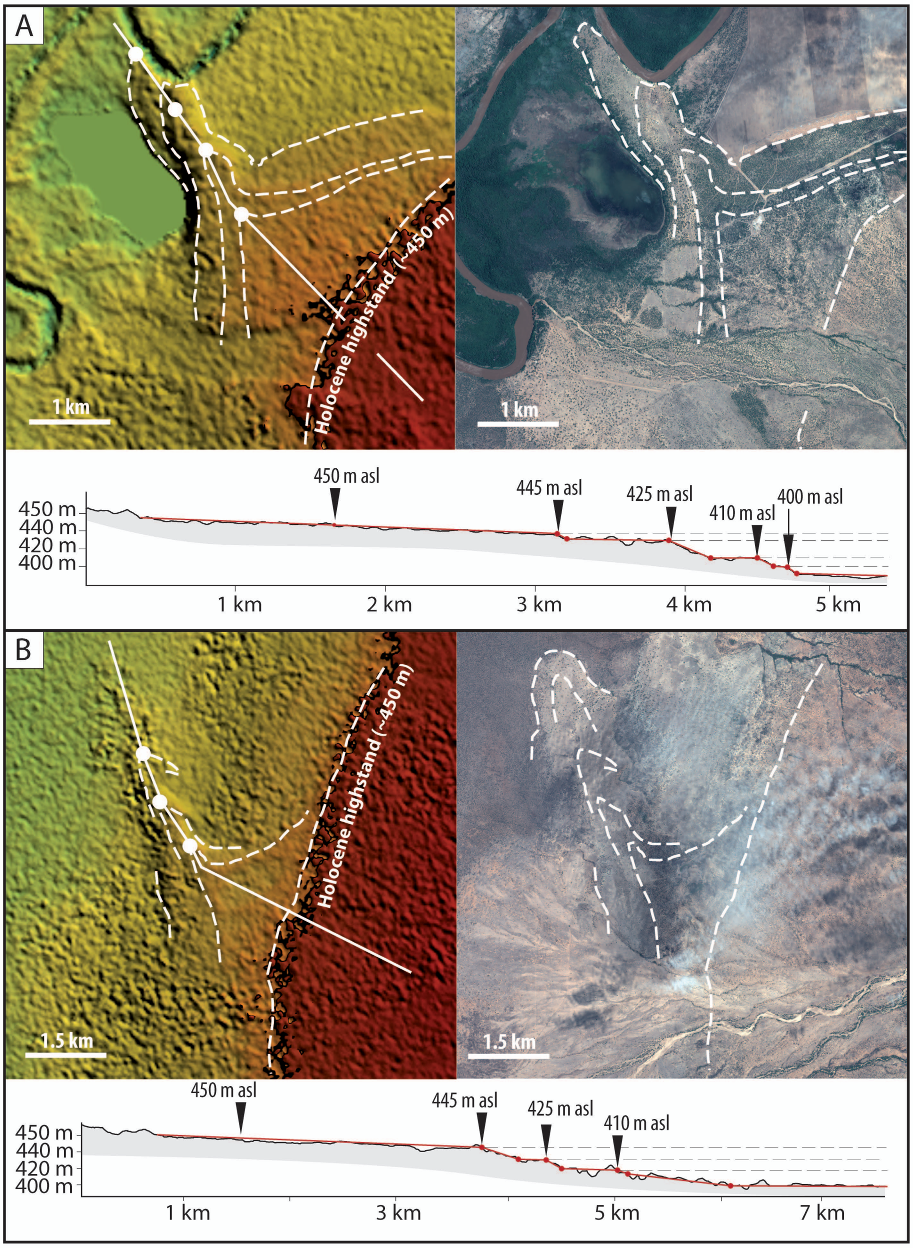
A
1 km
Holocene highstand (~450 m)
1 km
450 m asl
445 m asl
425 m asl
410 m asl
400 m asl
450 m
440 m
420 m
400 m
1 km
2 km
3 km
4 km
5 km
B
Holocene highstand (~450 m)
1.5 km
1.5 km
450 m asl
445 m asl
425 m asl
410 m asl
450 m
440 m
420 m
400 m
1 km
3 km
5 km
7 km

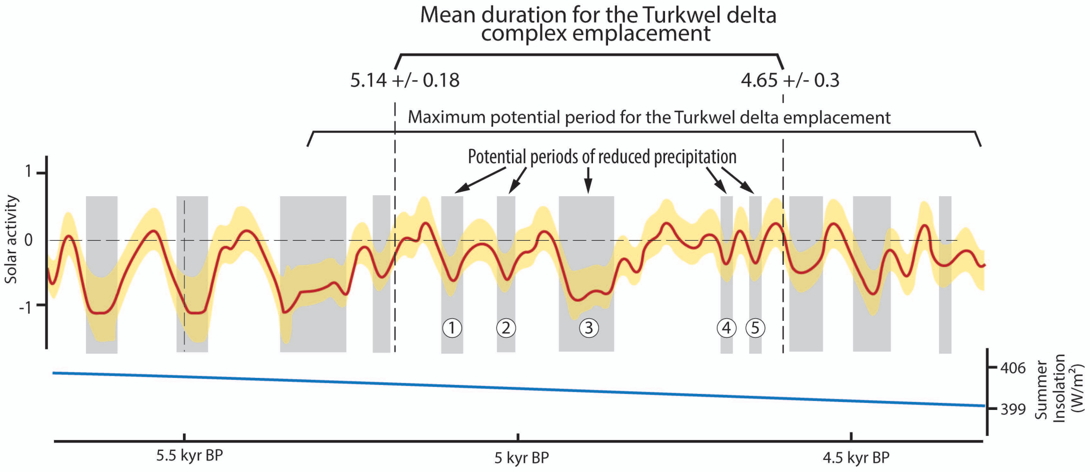
Mean duration for the Turkwel delta complex emplacement
5.14 +/- 0.18
4.65 +/- 0.3
Maximum potential period for the Turkwel delta emplacement
Potential periods of reduced precipitation
①
②
③
④
⑤
Solar activity
1
0
-1
406
399
Summer Insolation (W/m²)
5.5 kyr BP
5 kyr BP
4.5 kyr BP